Supplementary Information

An AIE-Active Multi-Stimuli Responsive Fluorophore with Solvatochromic, Acidochromic, and Ultrasensitive Cu^{2+}-Sensing Capabilities: Anti-Counterfeiting, Latent Fingerprint, Bioimaging and Food Samples Analysis

Pankaj Haloi[a], Ram Kumar Mandal[a], Abhinav Jain[a], Jebiti Haribabu[b], Daniel Moraga[c], Pranjit Barman[a] *

[a]Department of Chemistry, National Institute of Technology Silchar, Silchar, Cachar-788010 Assam

[b]Faculty of medicine, University of Atacama, Los Carreras 1579, 1532502, Copiapo, Chile

[c]Laboratorio de Fisiología, Departamento de Ciencias Biomédicas, Facultad de Medicina, Universidad de Tarapacá, Arica 1000000, Chile

***Author for correspondence:** Pranjit Barman

(**Email:** *barmanpranjit@yahoo.co.in*)

Table of Contents

List of Figures

1. Experimental Section

1.1 Reagents and Chemicals

The solvents employed in the spectral experiments were obtained from Sigma-Aldrich and were of spectrophotometric grade. The other chemicals used in this research were sourced from commercial suppliers and were used without further purification.

1.2 Instrumentation

The IR spectral data was recorded by Perkin Elmer MIR/FIR-FT-IR spectrophotometer. ^{1}H and ^{13}C nuclear magnetic resonance spectrums were recorded using a JEOL JNM ECS400 NMR spectrometer in $CDCl_3$ solvent at 400 MH_z. The chemical shift (δ) values were reported in ppm using TMS as reference standard. The ESI positive mass spectrum was taken from XEVOG2-XS QTOF spectrometer in DMSO solvent. UV-visible absorption spectrums were obtained by using a Cary 60 absorption spectrophotometer. A HITACHI-F4600 spectrophotometer was utilized to record the fluorescence emission spectrums.

1.3 Characterization

Yield: 90%; Pale yellowish-orange crystalline solid; melting point: 171-173°*C.*

FTIR (v, cm^{-1}): 3509 (O-H); 2998 (aromatic C-H); 1601 (C=N); 1436 (Aromatic C=C); 1151 (C-O) (**Fig. S1**).

^{1}H NMR (400 MHz, $CDCl_3$) (ppm): δ 12.99 (s, 1H), 9.40 – 9.32 (s, 1H), 7.17 – 6.93 (m, 11H), 2.85 – 2.79 (d, *J* = 0.5 Hz, 3H) (**Fig. S2**).

^{1}H NMR (400 MHz, CHLOROFORM-*D*) δ 9.40 – 9.32 (s, 1H), 7.17 – 6.93 (m, 11H), 2.85 – 2.79 (d, *J* = 0.5 Hz, 3H).

^{13}C NMR (126 MHz, DMSO-D_6) (ppm): δ 170.67, 165.22, 162.22, 158.05, 135.38, 131.58, 129.50, 129.34, 128.67, 128.52, 128.39, 122.80, 118.85, 114.23, 78.99 (**Fig. S3**).

ESI-Mass: Base peak was obtained at m/z = 329.45 $[(C_{16}H_{16}N_2O_2) + H]^+$ = 329.12] which confirmed the formation of the **HP** (**Fig. S4**).

1.4 Preparation of Stock Solutions

~1 mmol stock solutions of **HP** was prepared in four solvents having different polarity. For absorbance and emission analysis, the stock solutions of **HP** was diluted to a concentration of about ~50 μM in a suitable solvent. A combination of ~50 μM THF-water solution was prepared for aggregation investigations. To conduct pH tests, a 1 mmol stock solution was diluted to form

a ~50 μM concentration in 1:9 THF-aqueous buffer solution. The pH solution was made by the combination of Na_2HPO_4 and NaH_2PO_4 produced a 0.1 M phosphate buffer. The metal ion solutions of about ~10 mmol were developed in the water medium. Finally, the absorbance and emission spectrum were captured after 10 minutes of mixing [1].

1.5 Theoretical Calculations

The quantum chemical investigations were conducted using the GAUSSIAN 16 software [2]. The B3LYP 6-311g+(d, p) basis set was utilized for carrying out the optimization of the ground state configuration of **HP** [3]**.** But, for optimizing the ground state of the complexes of **HP,** the LanL2DZ basic set was selected [4].

1.6 Calculation of Quantum Yield

The fluorescence quantum yield was determined by utilizing Rhodamine B as the standard fluorophore [5].

$$\phi_u = \left(\frac{A_s F_u n_u^2}{A_u F_s n_s^2} \right) \phi_s$$

Where 'ϕ_u' is the quantum yield value of the unidentified fluorophore, 'ϕ_s' is the quantum yield value of the fluorophore taken as the standard reference (ϕ_s = 0.68 in ethanol medium). 'A_u' and 'A_s' are the absorbance values at the excitation wavelength for the unknown and the standard fluorophore, respectively. 'F_u' and 'F_s' are the integrated area of fluorescence intensity for the unknown and the standard fluorophore, respectively. 'n_u' and 'n_s' are the refractive index of the unknown and the standard fluorophore, respectively [6].

1.7 Determination of Limit of Detection (LOD)

The following equation was used to determine the LOD with the help of fluorescence titration,

$$LOD = 3\sigma/S$$

where σ stands for standard deviation value of blank measurements, and the S denotes slope of the calibration plot of I_0-I vs Cu^{2+} ion concentration, where I_0 & I were emission intensity of ligand in absence and presence of Cu^{2+} ions respectively.

1.8 Determination of Stern-Volmer constant (K_{sv})

The Stern-Volmer formula has been implemented to estimate the degree of fluorescence quenching caused by adding copper ions.

$$\frac{I_o}{I} = 1 + K_{SV} \times [Cu^{2+}]$$

Where, 'K_{sv}' is the Stern-Volmer constant, 'I_o' denotes the intensities of fluorescence in the absence of Cu^{2+} ions at different concentrations and 'I' represents intensities of fluorescence presence of Cu^{2+} ions at different concentrations [7].

1.9 Determination of Binding Constant (K_b)

Based on fluorometric titration data, binding constant (K_b) was determined by Benesi-Hildebrand equation,

$$\frac{1}{I - Io} = \left[\frac{1}{Imax - Io}\right]\left[\frac{1}{Kb.C} + 1\right]$$

where I_o denotes emission intensity of **HP** alone, I denote emission intensity of sensor **HP** in different equivalents of Cu^{2+} ions, I_{max} is emission intensity of senor **HP** when 2 equivalents of Cu^{2+} ions was added and C is copper ion concentration [8].

1.10 In-vitro cell culture

Hela cells were procured from National Centre for Cell Science (NCCS), Pune. For routine maintenance, cells were cultured in Dulbecco's Modified Eagle's Medium (DMEM) and incubated in a humidified atmosphere at 37 °C supplied with 5% CO_2.

1.11 Cell viability assay

Hela cells were treated with probe **HP** in varying concentration for 48 h. After the treatment, 3-(4,5-Dimethylthiazol-2-yl)-2,5-Diphenyltetrazolium Bromide (MTT) was added to each well and incubated for about 2 h. Following incubation period, the purple color formazon crystals formed were dissolved using DMSO. Colorimetric analysis was conducted using a multi-well plate reader (GloMax microplate reader, Promega) by measuring the absorbance at ~560 nm for the sample

and ~600 nm for background subtraction. Cell viability was calculated using the provided equation.

$$\textbf{\% of Cell viability} = \frac{(A_{570} - A_{600})_{Sample}}{(A_{570} - A_{600})_{Control}} \times 100$$

1.12 Cellular uptake study

For the uptake study, HeLa cells were cultured on coverslips in 6-well plates at a density of 1 × 10^5 cells/well and allowed to adhere for 24 h. After 24 h, cells were treated with probe **HP** for another 6 h. After the incubation period, the cells were washed with PBS and fixed with a 4% formaldehyde solution for 10 minutes. After fixation, the cells were washed again with PBS and examined using confocal microscopy (ZEISS LSM-880). For Copper ion sensing, following 6 h incubation, cells were exposed to Cu^{2+} for 30 mins and examined using confocal microscopy.

1.13 Preparation of Food Samples

For food sample preparation, fresh raw food materials were first processed using a juice mixer to obtain the corresponding food extracts. An aliquot of 5 mL of the prepared juice was transferred into a 10 mL autoclave digestion reactor. To this, 2.25 mL of concentrated nitric acid and 0.25 mL of 30% (v/v) hydrogen peroxide were carefully added. The sealed reactor was heated in an oven at 185 °C for 5 h to achieve complete digestion. After cooling, the resulting clear digest was diluted to a final volume of 25 mL using Tris-HCl buffer (pH 5) prior to analysis.

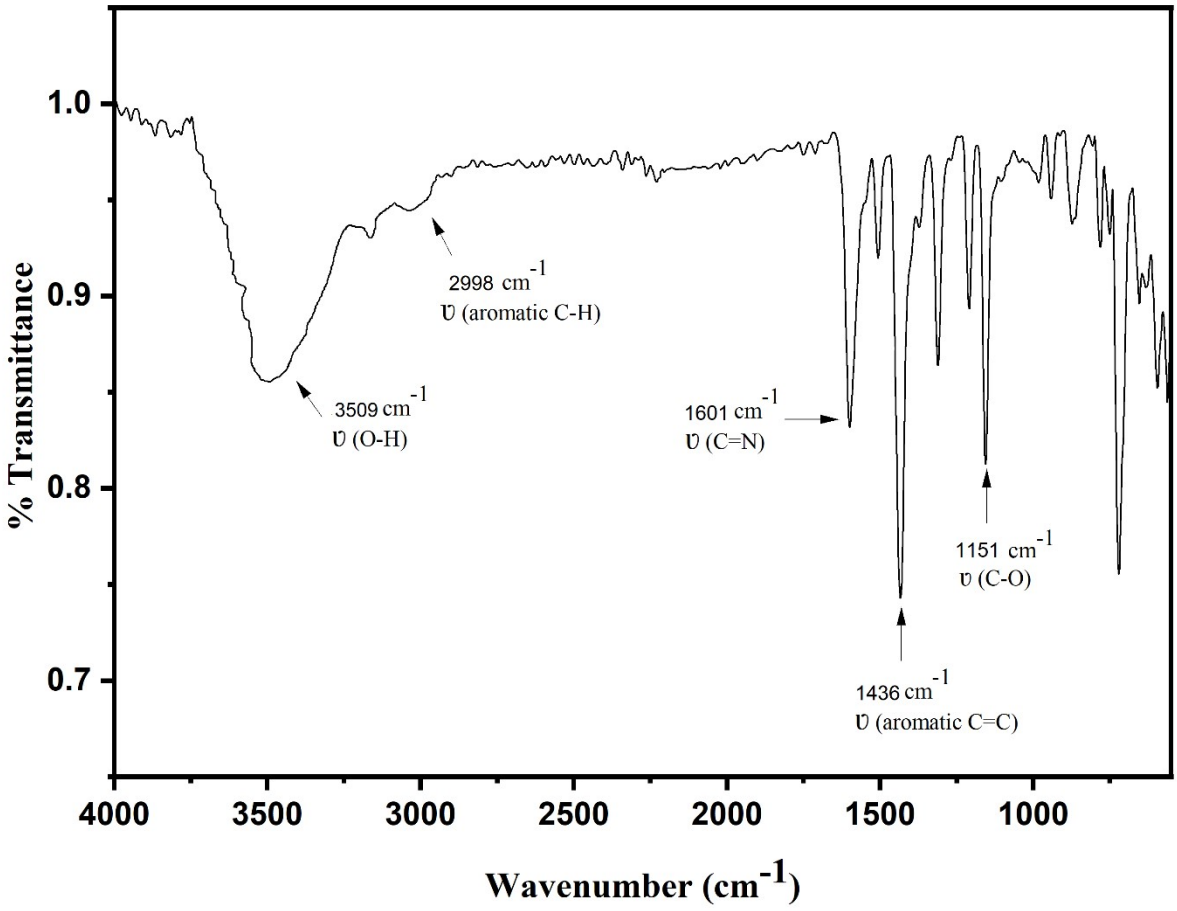

Fig. S1. FT-IR spectra of **HP**

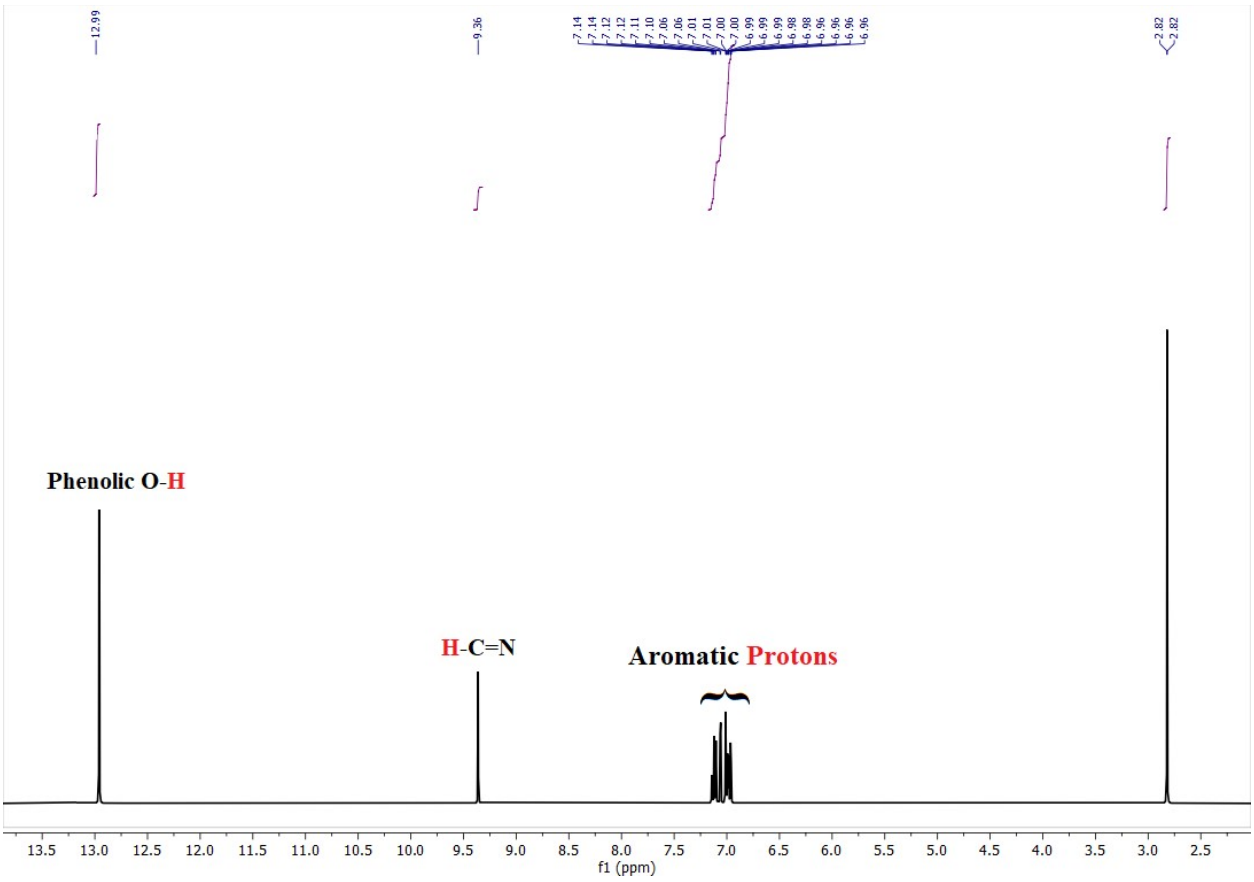

Fig. S2. ^{1}H-NMR spectra of **HP**

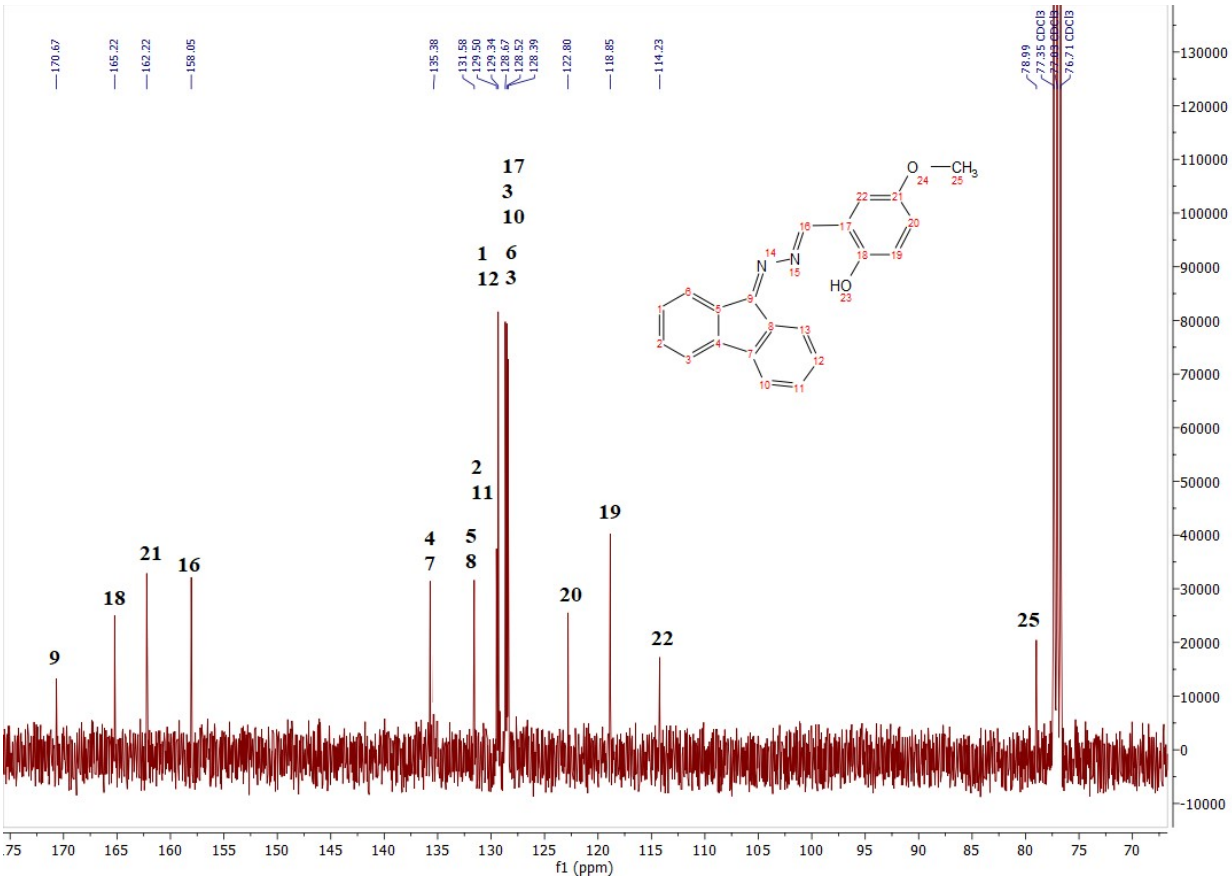

Fig. S3. ^{13}C-NMR spectra of **HP**

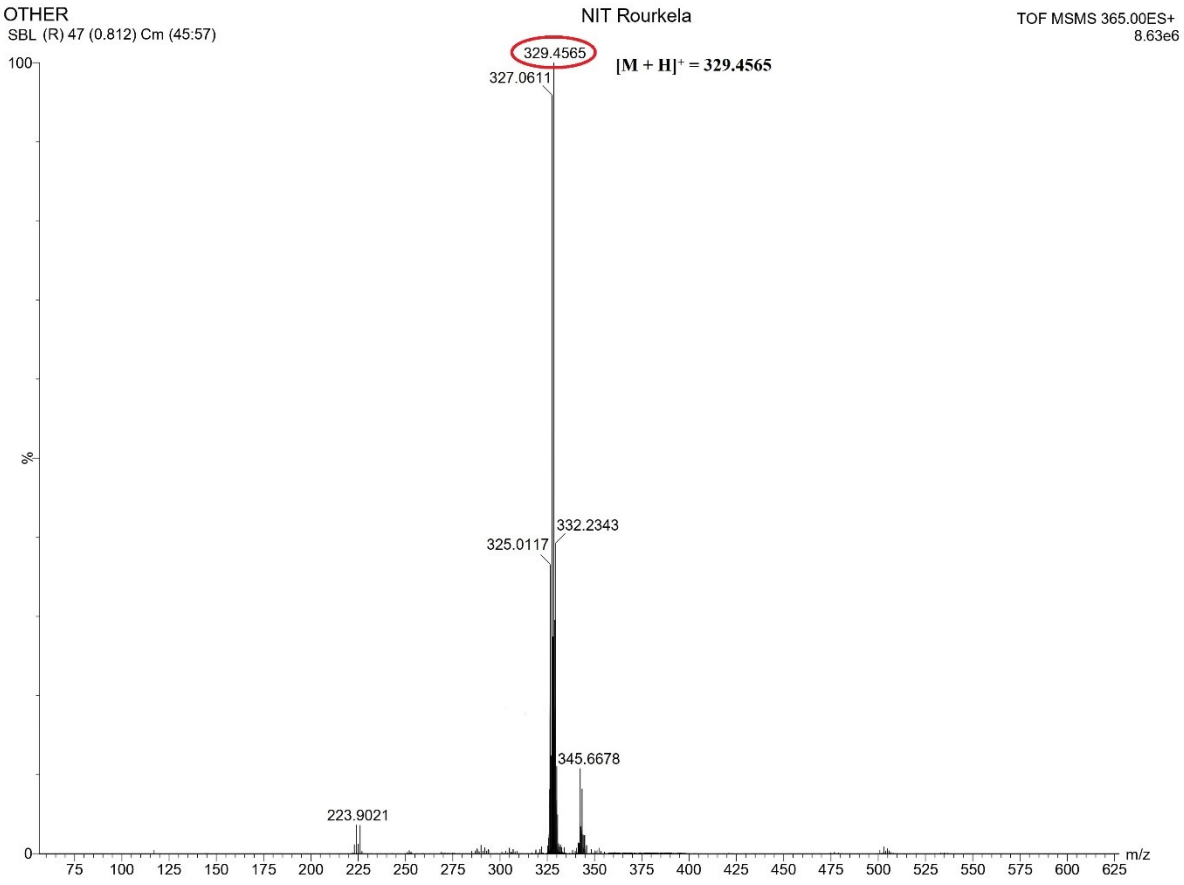

Fig. S4. ESI-MS spectra of **HP**

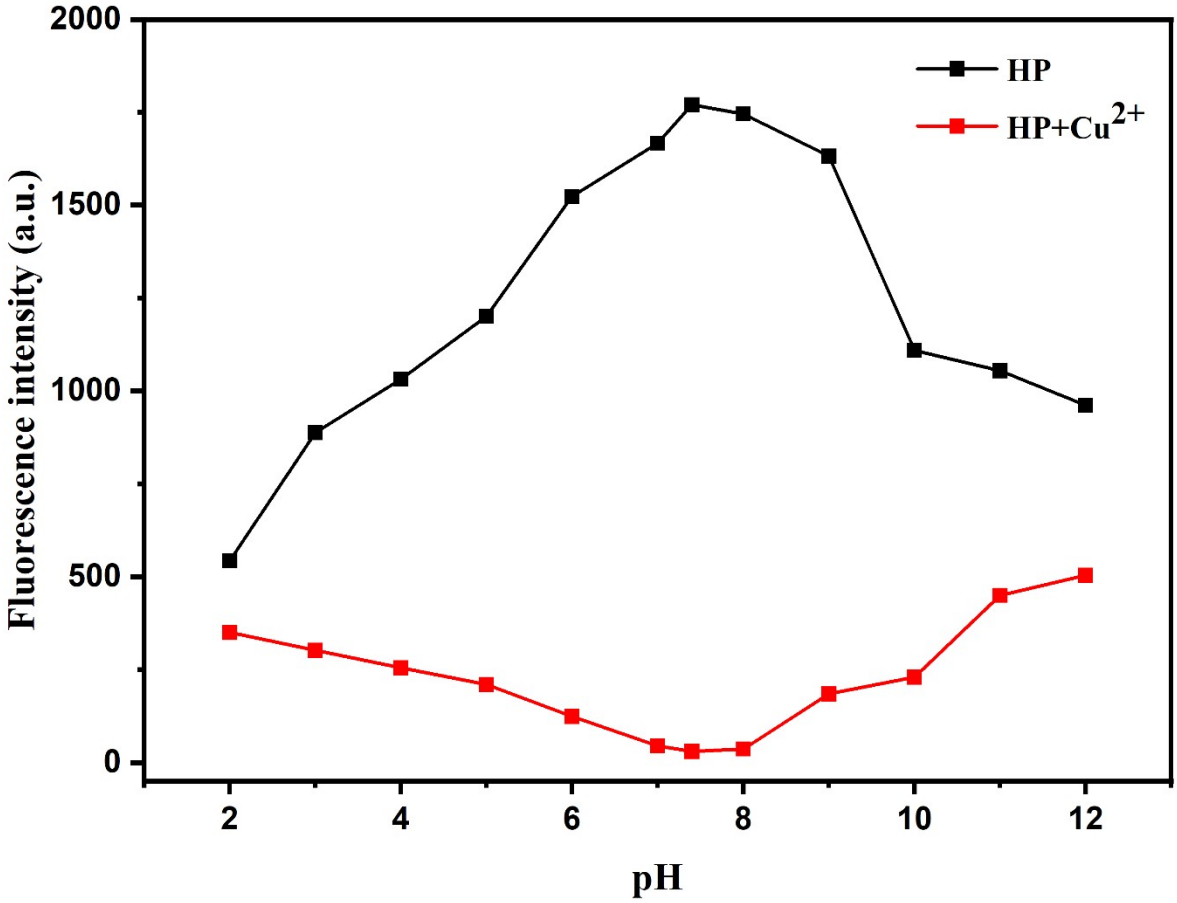

Fig. S5. Fluorescence spectra of **HP** with and without presence of copper in different pH

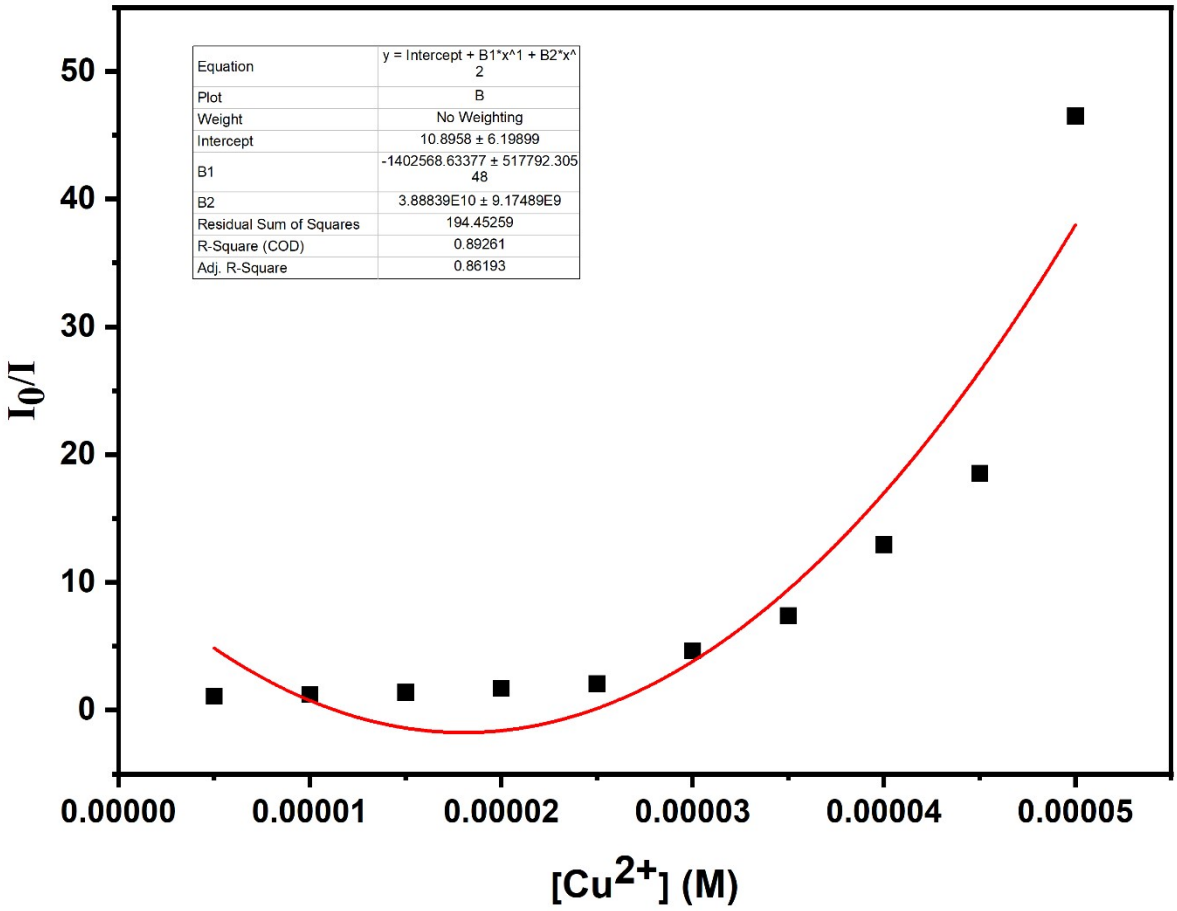

Fig. S6. Stern-volmer plot at high copper ion concentartion

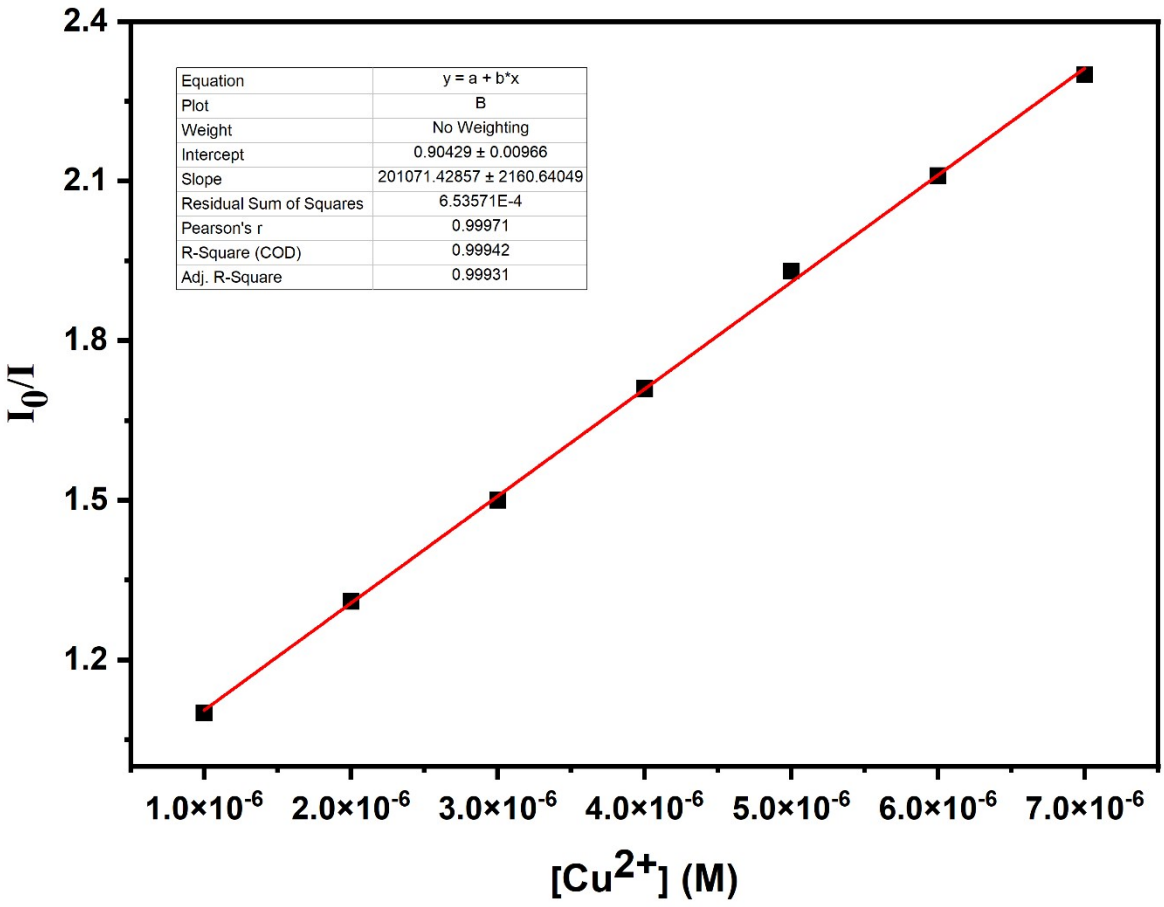

Fig. S7. Stern-volmer plot at low copper ion concentartion

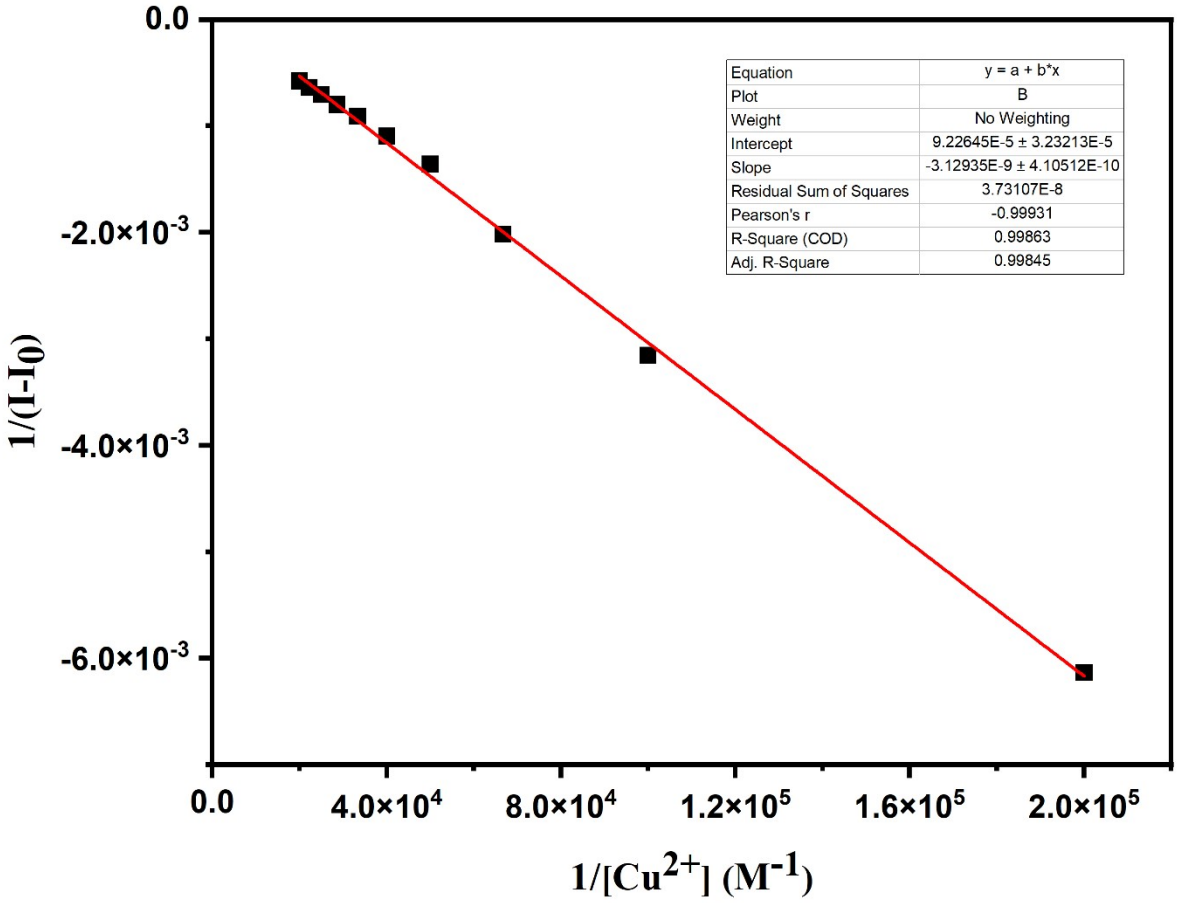

Fig. S8. BH-plot for binding contant determination

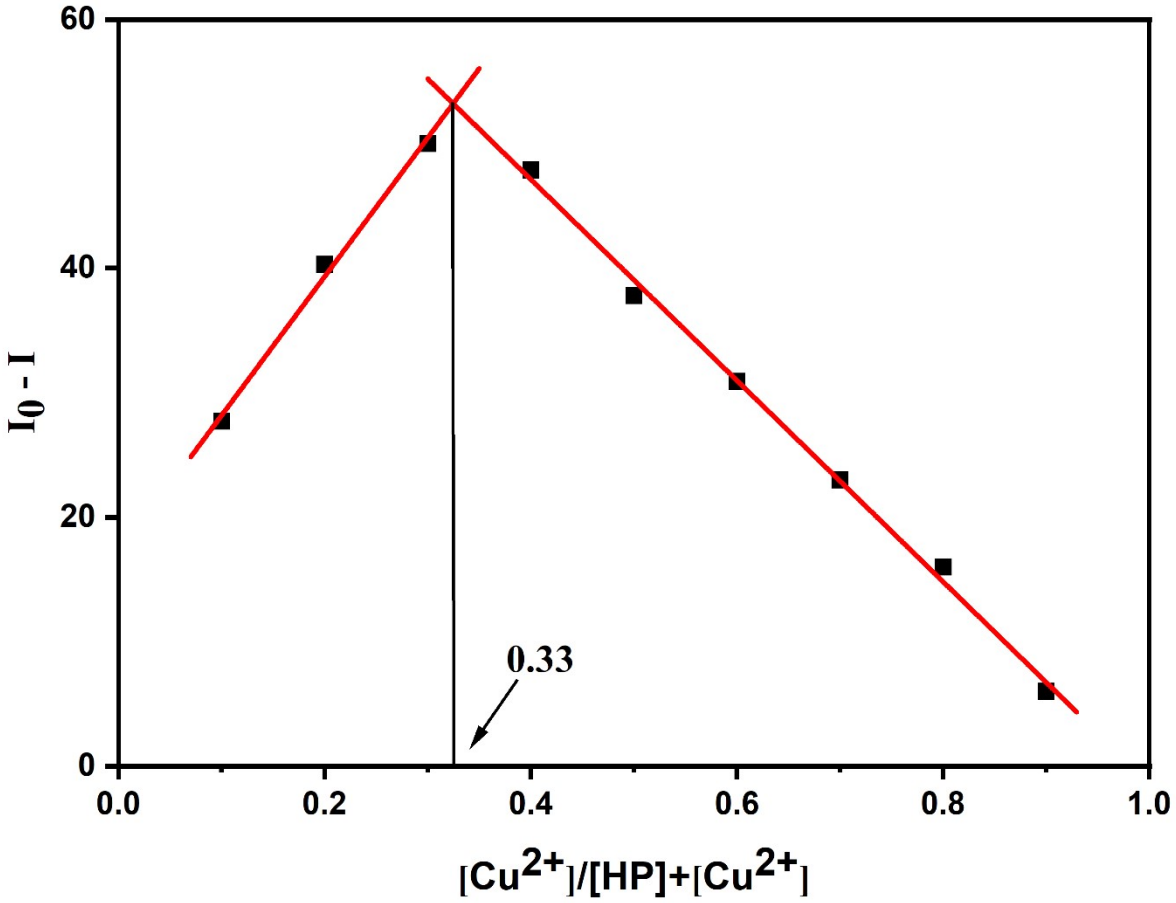

Fig. S9. Job's plot for binding stoichiometry determination

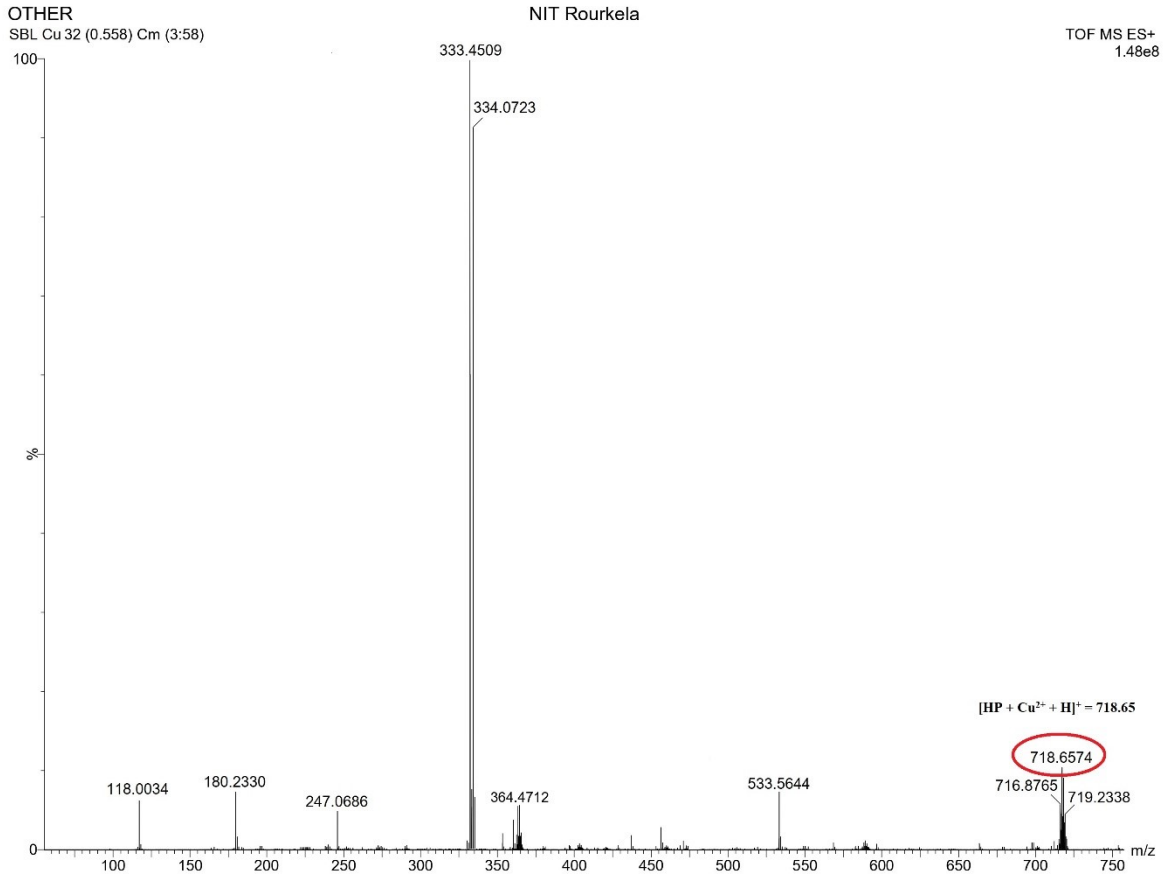

Fig. S10. ESI-MS spectra of **[HP+Cu^{2+}]** complex

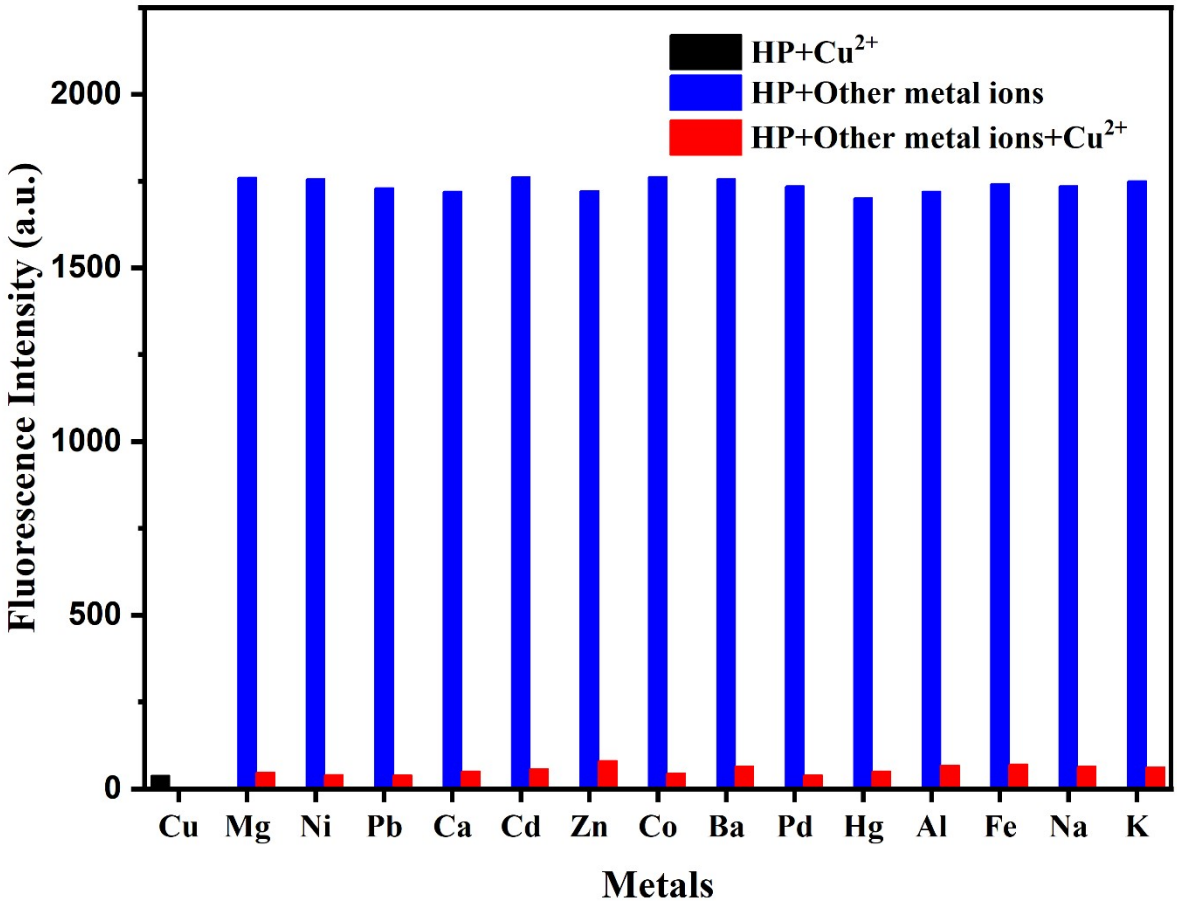

Fig. S11. Bar diagram illustrating the interference study of probe HP for Cu^{2+} (50µM) detection in the presence of various competing metal ions (100µM)

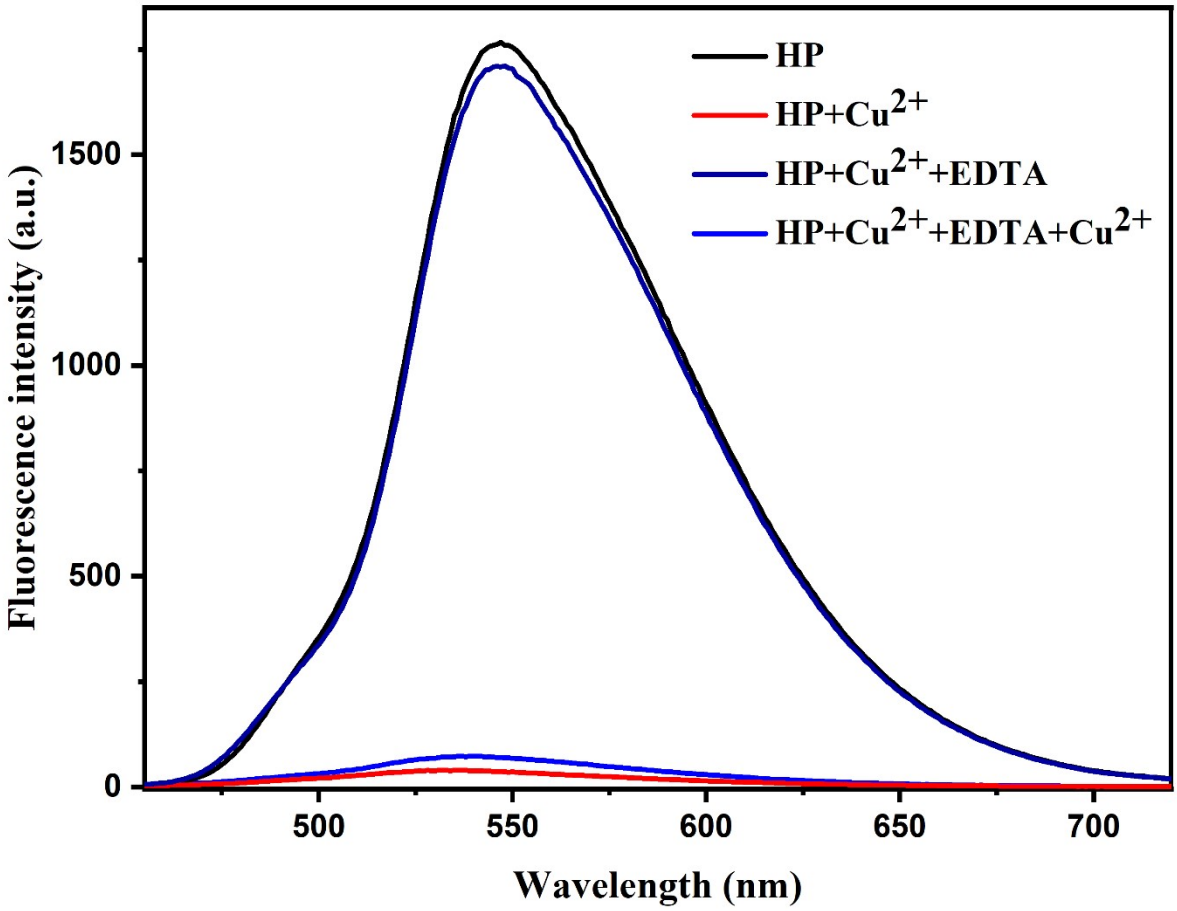

Fig. S12. Fluorescence spectra of reversibility study

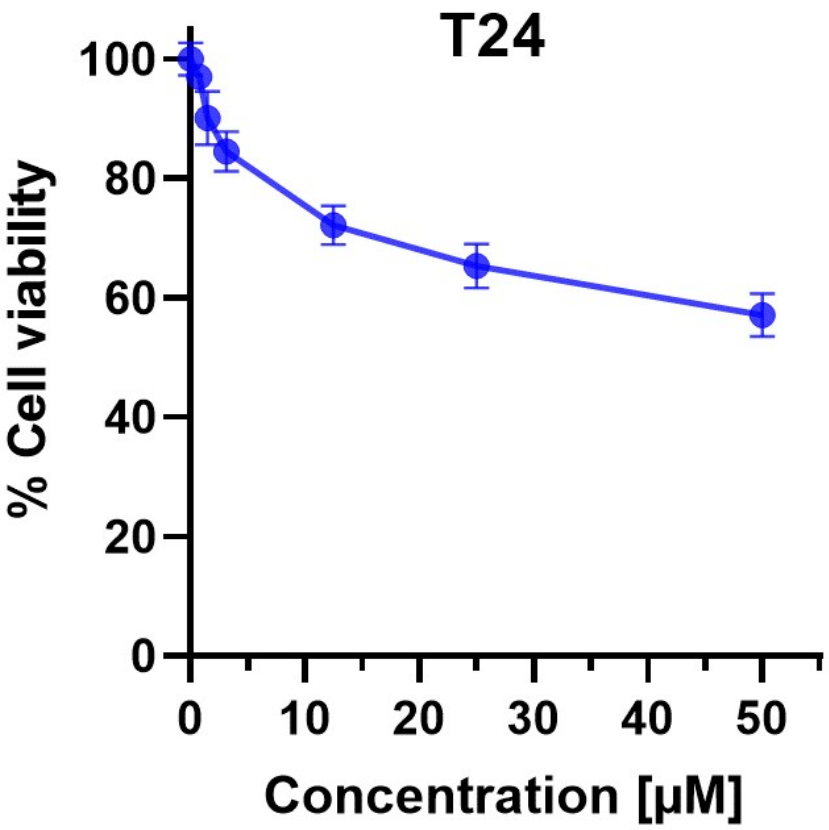

Fig. S13. Cell viability assay of probe **HP**

Table S1. A comparison of previously published sensors based on detection of Cu^{2+} ions.

S. No.	Chemosensor used	Solvent used	λ_{em} (nm)	LOD value (M)	Fluorescence strategy	Reference

1	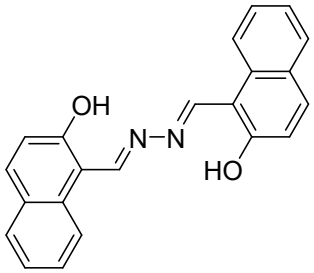	ACN-H_2O	530	10 x 10^{-9}	AIE-based turn-off	[9]
2	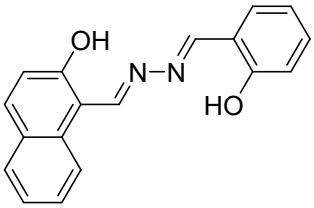	ACN-H_2O	534	200 x 10^{-9}	AIE-based turn-off	[9]
3	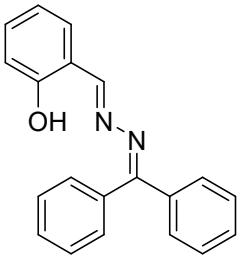	THF-H_2O	565	6.7 x 10^{-8}	AIE-based turn-OFF	[10]
4	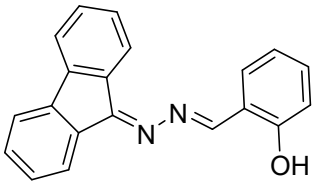	THF-H_2O	600	12.6 x 10^{-8}	AIE-based turn-OFF	[10]
5	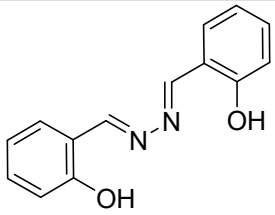	ACN-H_2O (1:9 v/v)	536	1 x 10^{-7}	AIE-based turn-off	[11]
6	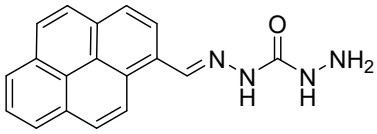	DMF-H_2O	430	35 x 10^{-9}	AEE turn ON	[12]

7	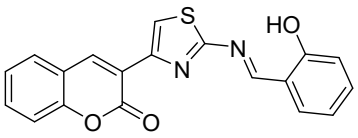	DMSO-HEPES buffer (2:8 v/v)	544	24 x 10^{-9}	AIE-based turn ON-OFF	[13]
8	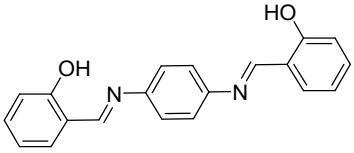	ACN-water (2:8 v/v)	549	5.90 x 10^{-5}	AIEE-ESIPT-TICT based Turn-OFF	[14]
9	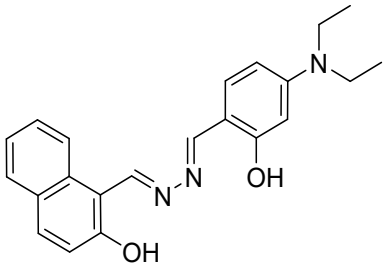	DMSO-H_2O-MeOH (0.1:1.9:8 v/v) HEPES buffer	464, 536	1.52 x 10^{-7}	TICT based turn-OFF	[15]
10	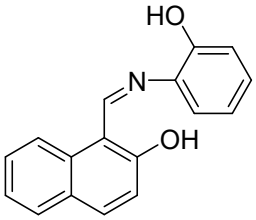	MeOH-H_2O (60% v/v)	516	57.2 x 10^{-9}	AIE-ESIPT based turn OFF-ON-OFF	[16]
11	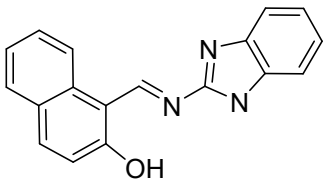	EtOH-PBS (1:1 v/v)	504	0.08 x 10^{-6}	AIE-ESIPT based turn OFF-ON-OFF	[17]
12	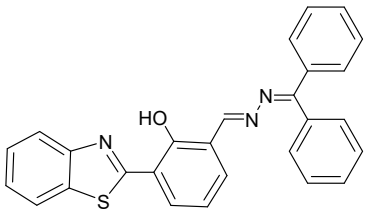	DMF-H_20 (1:9 v/v)	590	5.0 x 10^{-9}	ESIPT-TICT-AIE based turn-off	[18]

13	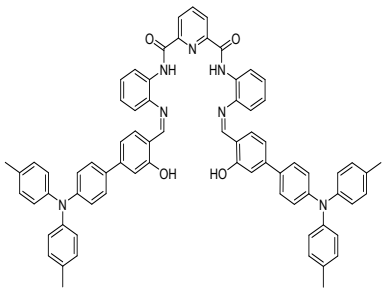	THF-H_2O	525-576	2.687 x 10^{-7}	AIE-ESIPT bases turn	[19]
14	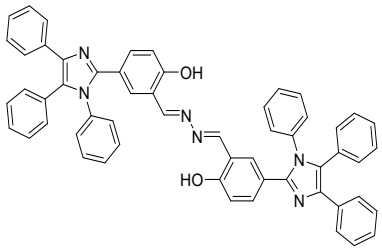	THF-H_2O (5/95, v/v)	550-560	8.3 x 10^{-7}	AIE based Turn OFF	[20]
15	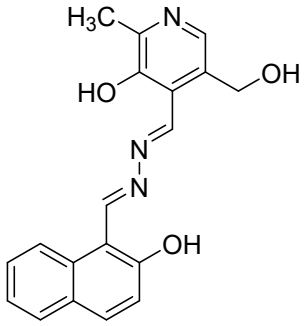	DMSO-HEPES, (40:60, v/v)	530, 570	32.9 x 10^{-9}	AIE-based turn OFF	[21]
16	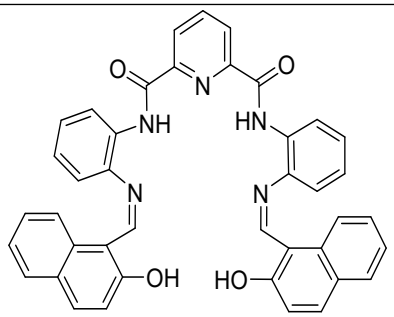	THF	588	1.8 x 10^{-7}	AIE-ESIPT based turn ON-OFF	[22]

17	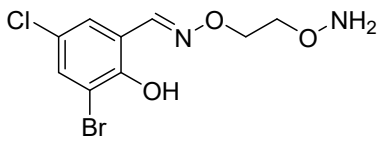	EtOH-H_2O	467	48.59 x 10^{-9}	AIE-based turn ON-OFF-ON	[23]
18	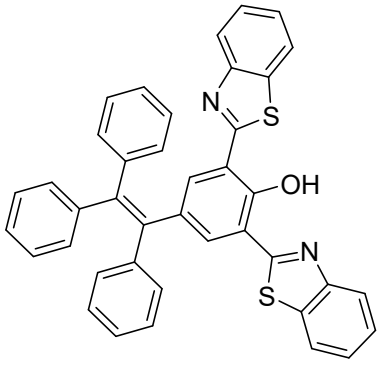	THF-water (1:9 v/v)	618	9.91 x 10^{-8}	AIE-ESIPT based turn ON-OFF	[24]
19	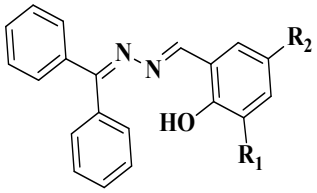 BSDPA: R_1 = H, R_2 = Br DBSDPA: R_1 = Br, R_2 = Br DTSDPA: R_1 = ditert, R_2 = ditert MSDPA: R_1 = H, R_2 = OMe	ACN-aq.buffer (1:9 v/v) pH 7.4 Phosphate buffer	560 to 600	5.4 x 10^{-9} -12.1 x 10^{-9}	AIE-ESIPT turn-OFF	[25]
20	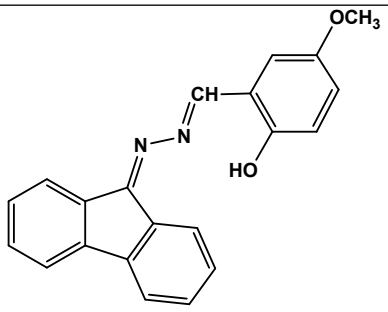	THF-water (1:9 v/v)	550	4.7 x 10^{-9}	AIE-based turn-OFF	This work

References:

[1] A. Jain, P. Saraswat, S. De, H. Roy, B. Nath, S.S. Ghosh, P. Barman, Position-induced

differential aggregation behavior with red-shifted emission: A case study of the promising copper ion sensor skeleton-based regio-isomers, J. Photochem. Photobiol. A Chem. 458 (2025) 115931.

[2] A. Schiafer, H. Horn, R. Ahlrichs, Fully optimized contracted Gaussian basis sets for atoms Li to Kr, J. Chem. Phys 97 (1992) 2571.

[3] A.D. Becke, Density-functional thermochemistry. III. The role of exact exchange, J. Chem. Phys. 98 (1993) 5648–5652.

[4] C.W. Bauschlicher Jr, H. Partridge, A modification of the Gaussian-2 approach using density functional theory, J. Chem. Phys. 103 (1995) 1788–1791.

[5] M.J. Snare, F.E. Treloar, K.P. Ghiggino, P.J. Thistlethwaite, The photophysics of rhodamine B, J. Photochem. 18 (1982) 335–346.

[6] M. Arshad, A. Paul, A. Joseph, Nanoscale detection of copper using an aggregation induced emission enhancement fluorescent sensor derived from hydroxy naphthaldehyde and benzyloxy benzaldehyde, J. Photochem. Photobiol. A Chem. 444 (2023) 114983.

[7] X.-J. Yan, Z.-G. Wang, Y. Wang, Y.-Y. Huang, H.-B. Liu, C.-Z. Xie, Q.-Z. Li, J.-Y. Xu, A dual-functional fluorescent probe for sequential determination of Cu2+/S2− and its applications in biological systems, Spectrochim. Acta Part A Mol. Biomol. Spectrosc. 243 (2020) 118797.

[8] J.R. Lakowicz, Instrumentation for fluorescence spectroscopy, in: Princ. Fluoresc. Spectrosc., Springer, 1999: pp. 25–61.

[9] B. Liu, H. Zhou, B. Yang, X. Hu, Aggregation–induced emission activity and further Cu2+-induced self-assembly process of two Schiff compounds, Sensors Actuators B Chem. 246 (2017) 554–562. https://doi.org/10.1016/j.snb.2017.02.120.

[10] Z. Wang, F. Zhou, C. Gui, J. Wang, Z. Zhao, A. Qin, B.Z. Tang, Selective and sensitive fluorescent probes for metal ions based on AIE dots in aqueous media, J. Mater. Chem. C 6 (2018) 11261–11265. https://doi.org/10.1039/C8TC03711F.

[11] H. Zhou, B. Yang, G. Wen, X. Hu, B. Liu, Assembly and disassembly activity of two

AIEE model compounds and its potential application, Talanta 184 (2018) 394–403. https://doi.org/10.1016/j.talanta.2018.03.007.

[12] W.-N. Wu, P.-D. Mao, Y. Wang, X.-J. Mao, Z.-Q. Xu, Z.-H. Xu, X.-L. Zhao, Y.-C. Fan, X.-F. Hou, AEE active Schiff base-bearing pyrene unit and further Cu2+–induced self-assembly process, Sensors Actuators B Chem. 258 (2018) 393–401. https://doi.org/10.1016/j.snb.2017.11.114.

[13] S.K. Padhan, N. Murmu, S. Mahapatra, M.K. Dalai, S.N. Sahu, Ultrasensitive detection of aqueous Cu 2+ ions by a coumarin-salicylidene based AIEgen, Mater. Chem. Front. 3 (2019) 2437–2447.

[14] N. Miengmern, A. Koonwong, S. Sriyab, A. Suramitr, R.P. Poo-arporn, S. Hannongbua, S. Suramitr, Aggregation-induced emission enhancement (AIEE) of N,N′-Bis(Salicylidene)-p-Phenylenediamine Schiff base: Synthesis, photophysical properties and its DFT studies, J. Lumin. 210 (2019) 493–500. https://doi.org/10.1016/j.jlumin.2019.02.023.

[15] R. Yadav, A. Rai, A.K. Sonkar, V. Rai, S.C. Gupta, L. Mishra, A viscochromic, mechanochromic, and unsymmetrical azine for selective detection of Al 3+ and Cu 2+ ions and its mitotracking studies, New J. Chem. 43 (2019) 7109–7119. https://doi.org/10.1039/C8NJ06413J.

[16] R. Das, S. Bej, H. Hirani, P. Banerjee, Trace-Level Humidity Sensing from Commercial Organic Solvents and Food Products by an AIE/ESIPT-Triggered Piezochromic Luminogen and ppb-Level “OFF–ON–OFF” Sensing of Cu 2+ : A Combined Experimental and Theoretical Outcome, ACS Omega 6 (2021) 14104–14121. https://doi.org/10.1021/acsomega.1c00565.

[17] W. Pan, X. Yang, Y. Wang, L. Wu, N. Liang, L. Zhao, AIE-ESIPT based colorimetric and “OFF-ON-OFF” fluorescence Schiff base sensor for visual and fluorescent determination of Cu2+ in an aqueous media, J. Photochem. Photobiol. A Chem. 420 (2021) 113506. https://doi.org/10.1016/j.jphotochem.2021.113506.

[18] A.A. Bhosle, S.D. Hiremath, A.C. Bhasikuttan, M. Banerjee, A. Chatterjee, Solvent-free

mechanochemical synthesis of a novel benzothiazole-azine based ESIPT-coupled orange AIEgen for the selective recognition of Cu2+ ions in solution and solid phase, J. Photochem. Photobiol. A Chem. 413 (2021) 113265. https://doi.org/10.1016/j.jphotochem.2021.113265.

[19] X. Zhang, S.-T. Wu, X.-J. Yang, L.-Y. Shen, Y.-L. Huang, H. Xu, Q.-L. Zhang, T. Sun, C. Redshaw, X. Feng, Dynamic Coordination between a Triphenylamine-Functionalized Salicylaldehyde Schiff Base and a Copper(II) Ion, Inorg. Chem. 60 (2021) 8581–8591. https://doi.org/10.1021/acs.inorgchem.1c00523.

[20] H. Wu, L. Lin, L. Zheng, H. Guo, F. Yang, Dual-response fluorescence sensor for detecting Cu2+ and Pd2+ based on bis-tetraphenylimidazole Schiff-base, J. Photochem. Photobiol. A Chem. 432 (2022) 114076. https://doi.org/10.1016/j.jphotochem.2022.114076.

[21] V. Bhardwaj, S.K. Ashok Kumar, S.K. Sahoo, Fluorescent sensing (Cu2+ and pH) and visualization of latent fingerprints using an AIE-active naphthaldehyde-pyridoxal conjugated Schiff base, Microchem. J. 178 (2022) 107404. https://doi.org/10.1016/j.microc.2022.107404.

[22] L. Shen, C.-J. Yu, H.-F. Xie, N. Xu, H. Xu, Y.-L. Huang, C. Redshaw, X. Feng, Q.-L. Zhang, Naphthaldehyde-based Schiff base dyes: aggregation-induced emission and high-contrast reversible mechanochromic luminescence, Mater. Chem. Front. 6 (2022) 2491–2498. https://doi.org/10.1039/D2QM00542E.

[23] Z.-F. Hu, Z.-L. Chai, Y.-R. Zheng, Y.-F. Ding, W.-K. Dong, Y.-J. Ding, A unique AIE multi-responsive half-salamo-like fluorescence sensor for temperature, pH and Cu2+/S2- ions in aqueous media, Microchem. J. 190 (2023) 108736. https://doi.org/10.1016/j.microc.2023.108736.

[24] Y. Pan, Y. Li, X. Sun, L. Tang, X. Yan, An “AIE+ESIPT” characteristic fluorescent probe for relay recognition of Cu2+ and H2S and its application in food samples and cell imaging, Dye. Pigment. 210 (2023) 110985. https://doi.org/10.1016/j.dyepig.2022.110985.

[25] A. Jain, S. De, P. Barman, Salicylaldehyde-diphenyl-azine skeleton-based ESIPT-coupled AIEgens with tunable emission and applicable as highly selective and sensitive Cu2+ ion sensor, Dye. Pigment. 220 (2023) 111769. https://doi.org/10.1016/j.dyepig.2023.111769.